An in Situ Attenuated Total Reflection Infrared Study of a Chiral Catalytic Solid−Liquid Interface: Cinchonidine Adsorption on Pt

Davide Ferri and Thomas Bürgi*

Contribution from the Laboratory of Technical Chemistry, Swiss Federal Institute of Technology, ETH Hönggerberg, CH-8093 Zürich, Switzerland

Received July 20, 2001

Abstract: An in situ attenuated total reflection study of the chiral solid−liquid interface created by cinchonidine adsorption on a Pt/Al_2O_3 model catalyst is presented. Experiments were performed in the presence of dissolved hydrogen, that is under conditions used for the heterogeneous enantioselective hydrogenation of α-functionalized ketones. Cinchonidine adsorbs via the quinoline moiety. The adsorption mode is coverage dependent and several species coexist on the surface. At low concentration (10^{-6}M) a predominantly flat adsorption mode prevails. At increasing coverage two different tilted species, α-H abstracted and N lone pair bonded cinchonidine, are observed. The latter is only weakly bound and in a fast dynamic equilibrium with dissolved cinchonidine. At high concentration (10^{-4}−10^{-3} M) all three species coexist on the Pt surface. A slow transition from an adsorbate layer with a high fraction of α-H abstracted cinchonidine to one with a high fraction of N lone pair bonded cinchonidine is observed with the cinchonidine concentration being the driving force for the process. The reverse transition in the absence of dissolved cinchonidine is fast. Cinchonidine competes with solvent decomposition products for adsorption sites on the Pt, which may contribute to the observed solvent dependence of the heterogeneous enantioselective hydrogenation of ketones by cinchonidine-modified Pt.

Introduction

Chiral modification of solid catalysts has gained considerable interest because it represents one of the most promising strategies for heterogeneous enantioselective catalysis.[1,2] Various approaches have been made to unravel fundamental aspects of chiral surfaces.[3−6] An easy, although efficient way to produce a chiral heterogeneous catalyst is through adsorption of a chiral modifier onto a catalytically active metal. Two such catalyst systems have been studied in some detail in the past: tartaric acid-modified Ni catalysts[7−9] for the hydrogenation of β-ketoesters and cinchona-modified Pt catalysts[10−12] for the hydrogenation of activated ketones. Although the scope of these reactions has steadily increased in the past few years the mechanism of enantiodifferentiation on the chiral surface is still a matter of active debate.[11,13−17] On the other hand, a thorough understanding of enantioselection is a prerequisite for rational development of these promising catalyst systems.

In the asymmetric hydrogenation of activated ketones the adsorption behavior of modifier and reactant, their conformation, and their intermolecular interaction are key issues, which need to be clarified to rationalize enantioselection. However, despite the wide literature on this reaction only little spectroscopic information is available to date on the adsorption behavior of reactant and modifier,[18−25] and the proposed mechanistic models thus largely rely on indirect information. This is partly due to the intrinsic complexity of the system. Furthermore, in situ spectroscopic studies of the solid−liquid interface are complicated by the presence of the solvent.

Adsorption of a cinchona alkaloid, 10,11-dihydrocinchonidine, has been investigated ex situ by XPS,[13,20] LEED,[20] NEXAFS,[21] and H/D isotope exchange studies.[19] Quinoline and 10,11-dihydrocinchonidine were found to adsorb preferentially flat through the π-aromatic system at room temperature, whereas

* Corresponding author. E-mail: buergi@tech.chem.ethz.ch. Telephone: +41-1-632 22 67. Fax: +41-1-632 11 63.

(1) Baiker, A.; Blaser, H. U. *Handbook of Heterogeneous Catalysis*; VCH: Weinheim, 1997; Vol. 5, p 2422.
(2) Baiker, A. *Curr. Opin. Solid State Mater. Sci.* **1998**, *3*, 86.
(3) McFadden, C. F.; Cremer, P. S.; Gellman, A. J. *Langmuir* **1996**, *12*, 2483.
(4) Ortega-Lorenzo, M.; Haq, S.; Bertrams, T.; Murray, P.; Raval, R.; Baddeley, C. J. *J. Phys. Chem. B* **1999**, *103*, 10661.
(5) Ortega-Lorenzo, M.; Baddeley, C. J.; Muryn, C.; Raval, R. *Nature* **2000**, *404*, 376.
(6) Attard, G. A. *J. Phys. Chem. B* **2001**, *105*, 3158.
(7) Izumi, Y. *Adv. Catal.* **1983**, *32*, 215.
(8) Webb, G.; Wells, P. B. *Catal. Today* **1992**, *12*, 319.
(9) Sugimura, T. *Catal. Surveys* **1999**, *3*, 37.
(10) Orito, Y.; Imai, S.; Niwa, S. *J. Chem. Soc. Jpn.* **1979**, 1118.
(11) Baiker, A. *J. Mol. Catal. A: Chem.* **1997**, *115*, 473.
(12) Blaser, H. U.; Jalett, H. P.; Müller, M.; Studer, M. *Catal. Today* **1997**, *37*, 441.
(13) Simons, K. E.; Meheux, P. A.; Griffiths, S. P.; Sutherlands, I. M.; Johnston, P.; Wells, P. B.; Carley, A. F.; Rajumon, M. K.; Roberts, M. W.; Ibbotson, A. *Recl. Trav. Chim. Pays Bas* **1994**, *113*, 465.
(14) Schwalm, O.; Minder, B.; Weber, J.; Baiker, A. *Catal. Lett.* **1994**, *23*, 271.
(15) Margitfalvi, J. L.; Hegedüs, M.; Tfirst, E. *Tetrahedron: Asymmetry* **1996**, *7*, 571.
(16) Augustine, R. L.; Tanielyan, S. K. *J. Mol. Catal. A: Chem.* **1996**, *112*, 93.
(17) Baiker, A. *J. Mol. Catal. A: Chem.* **2000**, *163*, 205.
(18) Sutherland, I. M.; Ibbotson, A.; Moyes, R. B.; Wells, P. B. *J. Catal.* **1990**, *125*, 77.
(19) Bond, G.; Wells, P. B. *J. Catal.* **1994**, *150*, 329.
(20) Carley, A. F.; Rajumon, M. K.; Roberts, M. W.; Wells, P. B. *J. Chem. Soc., Faraday Trans.* **1995**, *91*, 2167.
(21) Evans, T.; Woodhead, A. P.; Gutiérrez-Sosa, A.; Thornton, G.; Hall, T. J.; Davis, A. A.; Young, N. A.; Wells, P. B.; Oldman, R. J.; Plashkevych, O.; Vahtras, O.; Ågren, H.; Carravetta, V. *Surf. Sci.* **1999**, *436*, L691.
(22) Castonguay, M.; Roy, J. R.; Rochefort, A.; McBreen, P. H. *J. Am. Chem. Soc.* **2000**, *122*, 518.
(23) Bürgi, T.; Atamny, F.; Knop-Gericke, A.; Hävecker, M.; Schedel-Niedrig, T.; Schlögl, R.; Baiker, A. *Catal. Lett.* **2000**, *66*, 109.
(24) Bürgi, T.; Atamny, F.; Schlögl, R.; Baiker, A. *J. Phys. Chem. B* **2000**, *104*, 5953.
(25) Bonello, J. M.; Williams, F. J.; Santra, A. K.; Lambert, R. M. *J. Phys. Chem. B* **2000**, *104*, 9696.

10.1021/ja011769u CCC: $20.00
Published on Web 11/09/2001

at 323 K on average the quinoline ring was considerably tilted with respect to the surface.[21] However, these studies were performed in ultrahigh vacuum (UHV) and not under reaction conditions. In fact, to date virtually no spectroscopic information is available from the relevant chiral solid−liquid interface.

We have recently described the use of attenuated total reflection infrared spectroscopy (ATR-IR)[26] for the in situ study of the solid−liquid interface of a Pt/Al_2O_3 thin film model catalyst.[27] Through CO adsorption it has been shown that the Pt can be cleaned by O_2- and H_2-saturated solvent. CO adsorption onto the Pt/Al_2O_3 thin film strongly resembled the one of commercial Pt-based catalysts. Also, scanning tunneling microscopy (STM) showed that the Pt film consists of densely packed Pt particles of similar size (a few nm) as found on commercial supported Pt catalysts. We have furthermore demonstrated in a preliminary communication that the sensitivity of the ATR technique is good enough to detect the modifier, which is a weak infrared absorber, at the solid−liquid interface.[28] Here we report a detailed in situ spectroscopic study of the chiral solid−liquid interface generated by adsorption of cinchonidine on Pt.

Experimental Section

Materials. Cinchonidine (Fluka, 98%), quinoline (Fluka, ≥97%), quinuclidine (Fluka, >97%), 1,2,3,4-tetrahydroquinoline (1THQ, Fluka, ~95%), 5,6,7,8-tetrahydroquinoline (5THQ, TCI, >95%), *cis-trans*-decahydroquinoline (DHQ, Aldrich, 97%), pyridine (Fluka, ≥99%), 2-methylquinoline (Acros, 97%), and cyclohexane (technical grade) were used as received. If not otherwise specified, millimolar (10^{-3} M) solutions were prepared using dichloromethane solvent (Baker) stored over 5 Å molecular sieves. The gases supplied by PANGAS were N_2 (99.995 vol %) and H_2 (99.999 vol %).

Film Preparation. The Pt/Al_2O_3 thin films were prepared directly on a Ge internal reflection element (IRE) by physical vapor deposition. Al_2O_3 and Pt targets were heated with an electron beam as described in detail elsewhere.[27] First, 100 nm Al_2O_3 were deposited followed by 1 nm Pt. The 25-reflections Ge IRE was polished before each film deposition by means of a 0.25 μm diamond paste and rinsed with ethanol.

Spectroscopy. In situ ATR-IR spectra were recorded on a Bruker IFS-66 spectrometer equipped with a commercial ATR accessory (Wilks Scientific) and a liquid nitrogen-cooled MCT detector by co-adding 200 scans at 4 cm^{-1} resolution. After cell mounting and optics alignment the probe chamber was purged with dried air overnight.

N_2-saturated solvent (CH_2Cl_2 or cyclohexane) was circulated over the thin film by means of a microdosing pump for about 2 h to stabilize the signal. The homemade stainless steel flow-through cell was cooled at 283 K using a thermostat throughout the experiments. Before adsorption the Pt film was treated with H_2-saturated solvent for 10 min. We have shown recently that this procedure cleans the Pt surface.[27] An H_2-saturated solution of the molecule under investigation at the desired concentration was then pumped through the cell.

Cinchonidine adsorption isotherm was determined by admitting solutions of the alkaloid in CH_2Cl_2 at concentrations ranging from 10^{-6} to 10^{-4}M at 283 K. Stabilization of the IR signal was allowed before admission of the next solution at higher concentration.

ATR spectra are presented in absorbance units with the last spectrum recorded during cleaning serving as the reference. Where needed, signals from the water gas-phase spectrum in the 1700−1400 cm^{-1} range were subtracted.

IR transmission spectra of CH_2Cl_2 solutions and pure liquids were collected with the same instrument but with a DTGS detector by co-adding 200 scans at 4 cm^{-1} resolution using a 1 mm path length CaF_2 cell.

Calculations. Quantum chemical calculations were performed by using the GAUSSIAN98[29] set of programs. A density functional hybrid method with Becke's three-parameter functional and the nonlocal correction of Perdew and Wang (B3PW91)[30] was applied to calculate vibrational frequencies of quinoline and quinuclidine after complete structure optimization. The triple-ζ version of Dunning's correlation consistent basis set was used.[31]

Results

Chemistry of CH_2Cl_2 on Pt/Al_2O_3. To understand the features in the ATR spectra the chemistry of the solvent has to be considered. The solvent and its decomposition products will be partially removed from the metal−liquid interface upon adsorption of a molecule, leaving their signals in the resulting spectra. Therefore, we first present some results on the interaction of CH_2Cl_2 with Pt, which was studied by contacting the Pt/Al_2O_3 film with a solution of CH_2Cl_2 in cyclohexane. The cleaning procedure for Pt using H_2-saturated solvent[27] proved effective also with cyclohexane. Removal of carbonate species identified by strong negative signals at 1538 and 1396 cm^{-1} could be observed. When CH_2Cl_2 was allowed to contact the cleaned Pt surface by admitting a 0.1 M solution in H_2-saturated cyclohexane at 283 K, a broad positive band at 1399 cm^{-1} dominated the ATR spectrum in the 1000−2000 cm^{-1} region. Strong negative signals at 2930 and 2850 cm^{-1} (C−H stretching) and 1450 cm^{-1} (CH_2 scissoring) indicated displacement of cyclohexane from the metal−liquid interface upon admission of CH_2Cl_2.

The rich chemistry of haloalkanes has been studied on a variety of transition metals under UHV conditions,[32] and it has recently been reported that CH_2Cl_2 decomposes on adsorption on Pt/Al_2O_3 catalysts by breaking one or both C−Cl bonds.[33] Hydrocarbons (CH_4 and ethylene) and HCl were found to form. Since CH_2Cl_2 does not show appreciable adsorption on Pt(111) under UHV conditions[34] we assign the signal at 1399 cm^{-1} to methylene species (eventually Cl-containing) arising from CH_2Cl_2 decomposition on Pt. Upon adsorption of molecules from CH_2Cl_2 on the Pt/Al_2O_3 film a strong negative band was observed at 1399 cm^{-1}, indicating displacement of methylene species (see for example Figure 1) together with negative bands at 1338 and 1120 cm^{-1} associated with ethylidyne ($\equiv C-CH_3$). The latter can be formed by recombination of methylene[33] and also methyl[35] species. Adsorption of molecules from the cyclohexane solution did not yield these signals, thus supporting their assignment, since for cyclohexane no decomposition to $=CH_2$ and $\equiv C-CH_3$ is expected.

(26) Harrick, N. J. *Internal Reflection Spectroscopy*; Interscience Publishers: New York, 1967.
(27) Ferri, D.; Bürgi, T.; Baiker, A. *J. Phys. Chem. B* **2001**, *105*, 3187.
(28) Ferri, D.; Bürgi, T.; Baiker, A. *J. Chem. Soc., Chem. Commun.* **2001**, 1172.
(29) Frisch, M. J.; Trucks, G. W.; Schlegel, H. B.; Scuseria, G. E.; Robb, M. A.; Cheeseman, J. R.; Zakrzewski, V. G.; Montgomery, J. A., Jr.; Stratmann, R. E.; Burant, J. C.; Dapprich, S.; Millam, J. M.; Daniels, A. D.; Kudin, K. N.; Strain, M. C.; Farkas, O.; Tomasi, J.; Barone, V.; Cossi, M.; Cammi, R.; Mennucci, B.; Pomelli, C.; Adamo, C.; Clifford, S.; Ochterski, J.; Petersson, G. A.; Ayala, P. Y.; Cui, Q.; Morokuma, K.; Malick, D. K.; Rabuck, A. D.; Raghavachari, K.; Foresman, J. B.; Cioslowski, J.; Ortiz, J. V.; Baboul, A. G.; Stefanov, B. B.; Liu, G.; Liashenko, A.; Piskorz, P.; Komaromi, I.; Gomperts, R.; Martin, R. L.; Fox, D. J.; Keith, T.; Al-Laham, M. A.; Peng, C. Y.; Nanayakkara, A.; Gonzalez, C.; Challacombe, M.; Gill, P. M. W.; Johnson, B.; Chen, W.; Wong, M. W.; Andres, J. L.; Gonzalez, C.; Head-Gordon, M.; Replogle, E. S.; Pople, J. A. *Gaussian98*, rev. A.7; Gaussian Inc.: Pittsburgh, PA, 1998.
(30) Becke, A. D. *J. Chem. Phys.* **1993**, *98*, 5648.
(31) Woon, D. E.; Dunning, T. H. *J. Chem. Phys.* **1993**, *98*, 1358.
(32) Bent, B. E. *Chem. Rev.* **1996**, *96*, 1361.
(33) Toukoniity, E.; Mäki-Arvela, P.; Villela, A. N.; Neyestanaki, A. K.; Salmi, T.; Leino, R.; Sjöholm, R.; Laine, E.; Väyrynen, J.; Ollonqvist, T.; Kooyman, P. J. *Catal. Today* **2000**, *60*, 175.
(34) Garwood, G. A.; Hubbard, A. T. *Surf. Sci.* **1982**, *118*, 223.
(35) Fairbrother, D. H.; Peng, X. D.; Viswanathan, R.; Stair, P. C.; Trenary, M.; Fan, J. *Surf. Sci. Lett.* **1993**, *285*, L455.

Table 1. Vibrational Frequencies of Cinchonidine, Quinoline, and Quinuclidine in Solution (or neat) and Adsorbed on Pt/Al_2O_3

cinchonidine		quinoline				quinuclidine				
IR[b]	Pt[d] (283 K)	IR[c]	calcd	symmetry(C_s)	Pt[d] (283 K)	IR[b]	calcd	symmetry (C_{3v})	Pt[d] (283 K)	assignment
1321	**1318**[e]	1314	1371	A_1	~**1310**					ring stretch
1321	**1318**[e]					1320	1348	A_1	**1323**	δ(C−H)
1321						1320	1353	e		ω(C−H)
1345						1345	1372	e		δ(C−H)
1351	**1355**[e]					1353	1379	A_1	**1341**	δ(C−H)
1383						1377	n.o.	A_1+A_2+e	**1372**	overtone[f]
1383		1371	1406	A_1						ring stretch
1394		1392	1424	A_1						ring stretch
n.o.	**1421**[e]	1431	1470	A_1						ring stretch
1454	**1458**[1,2,3]					1454	1485	A_1	**1461**	δ(C−H)
1454						1454	1489	e		δ(C−H)
1463	**1458**[1,2,3]					1463	1505	A_1	**1461**	δ(C−H)
1463		1469	1505	A_1						ring stretch
1509	**1511**[3]	1500	1548	A_1	**1507**[3]					ring stretch
1570	**1530**[2]				**1540**[3]					α-quinolyl
1570	~**1570**[1,2,3]	1569	1618	A_1	**1569**[1,2,3]					ring stretch
1593	**1590**[3]	1594	1651	A_1	**1592**[3]					ring stretch
1615	**1610**[3]	1620	1673	A_1	**1620**[3]					ring stretch
1635										ν(C═C)

[a] Calculated frequencies and assignments are also given. For adsorbed cinchonidine and quinoline different species (***1***, ***2***, ***3***) are observed. ***1*** = flat adsorbed, ***2*** = α-quinolyl, and ***3*** = N lone pair bonded species, see Scheme 2 and text. n.o. = not observed. [b] IR spectrum of a 0.01 M solution in CH_2Cl_2. [c] IR spectrum of neat liquid. [d] Adsorption from CH_2Cl_2 solvent. [e] Adsorption from cyclohexane. [f] See ref 38.

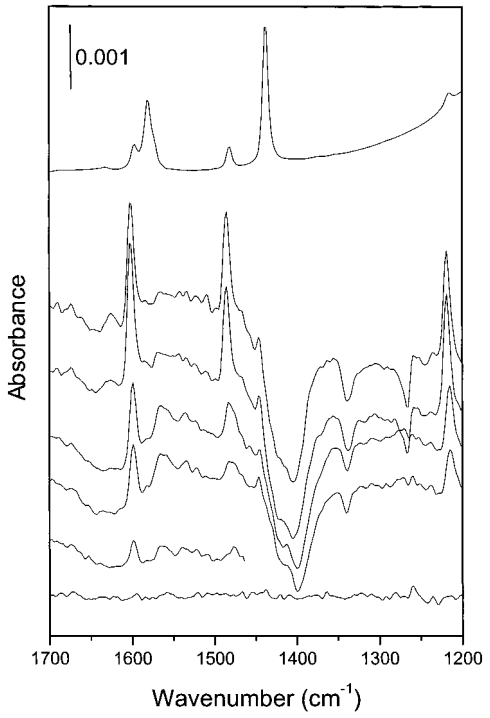

Figure 1. ATR spectra of pyridine (Py) adsorbed on Pt/Al_2O_3-coated Ge internal reflection element from H_2-saturated CH_2Cl_2. Conditions: $C_{Py} = 10^{-3}$ M; $T = 283$ K. Spectra recorded after (from bottom to top) 0, 2, 4, 8, 23, and 83 min contact time are shown. The top trace shows a scaled transmission spectrum ($C_{py} = 0.01$ M in CH_2Cl_2) for comparison.

Adsorption of Pyridine. Pyridine can be viewed as a model for the quinoline part of the cinchonidine modifier, which was proposed to act as its anchor.[11] Furthermore, pyridine adsorption on Pt has been well-studied under UHV conditions so that it can be used as reference. Figure 1 shows ATR spectra of pyridine adsorbed from H_2-saturated CH_2Cl_2 on the Pt/Al_2O_3 film at 283 K. For comparison a scaled transmission spectrum of neat pyridine is also shown. Strong perturbation of the intensity and position of the characteristic bands of pyridine upon adsorption on the Pt film is obvious. At low coverage

Scheme 1. Chemical Structure of Cinchonidine, Quinuclidine and Quinoline[a]

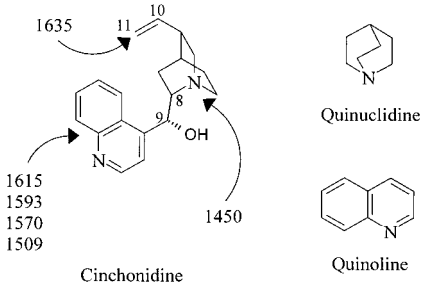

[a] IR frequencies (cm^{-1}) of cinchonidine vibrations in the 1650−1400 cm^{-1} range (determined from the transmission IR spectrum of a 0.01 M solution in CH_2Cl_2) are also given.

(low contact time) signals at 1598, 1564, 1539, 1477, 1445, and 1214 cm^{-1} and at 1068 and 1041 cm^{-1} (not shown) have been observed. The signals at 1598, 1477, and 1214 cm^{-1} shifted toward 1601, 1485, and 1218 cm^{-1} and were enhanced at high coverage. Also, a new signal slowly appeared at 1625 cm^{-1}, whereas the signal at 1564 cm^{-1} was attenuated. On flowing the neat solvent the signals disappeared, and only very weak bands at 1566 and 1485 cm^{-1} could be detected. The negative signals at 1264 cm^{-1}, ca. 1400, and 1338 cm^{-1} are due to removal of solvent and solvent decomposition products from the interface as detailed later.

Adsorption of Cinchonidine. The structure of the alkaloid cinchonidine is shown in Scheme 1. The 1650−1450 cm^{-1} spectral region of the solution spectrum displays signals corresponding to vibrational modes of the vinyl (ν(C═C), 1635 cm^{-1}), quinoline (ring modes, 1615, 1593, 1570, and 1509 cm^{-1}) and quinuclidine (1454 cm^{-1}) moieties (see also Table 1 for assignments).

Figure 2 shows ATR spectra recorded after contacting the Pt/Al_2O_3 film with a 10^{-3} M solution of cinchonidine in CH_2Cl_2. For comparison a scaled transmission spectrum of a 0.01 M solution is also given. Note that contacting the bare Al_2O_3 film with a cinchonidine solution did not show significant signals from adsorbed species. Also, no adsorption was observed when contacting the Pt/Al_2O_3 film with cinchonidine before cleaning

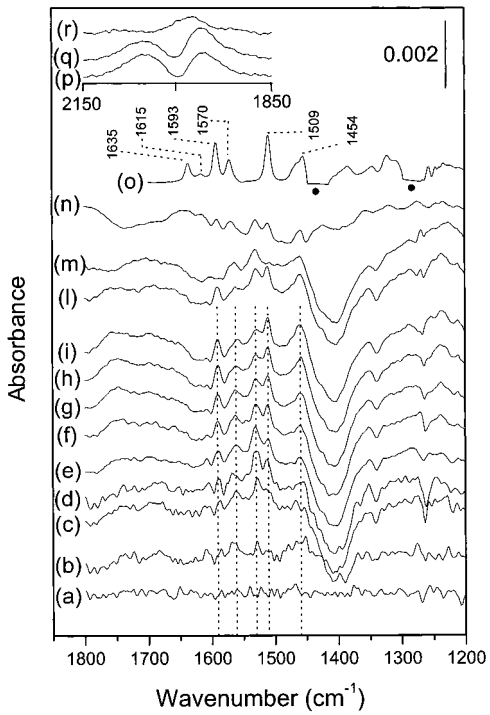

Figure 2. ATR spectra of cinchonidine (CD) on Pt/Al_2O_3-coated Ge IRE at 283 K adsorbed from H_2-saturated CH_2Cl_2 (C_{CD}= 10^{-3} M, traces a−i) and H_2-saturated cyclohexane (C_{CD} = 10^{-4} M, trace n). Spectra were recorded at 0, 0.6, 1.3, 2, 3, 22, 42, 82, and 122 min (traces a−i). Traces l and m were recorded while flowing N_2-saturated CH_2Cl_2 after cinchonidine adsorption. (o) Scaled (1:80) transmission spectrum (C_{CD} = 0.01M); uncompensated solvent (●). The inset shows the 2150−1850 cm^{-1} spectral region with trace p, q, and r being the extension of trace e, i, and m, respectively.

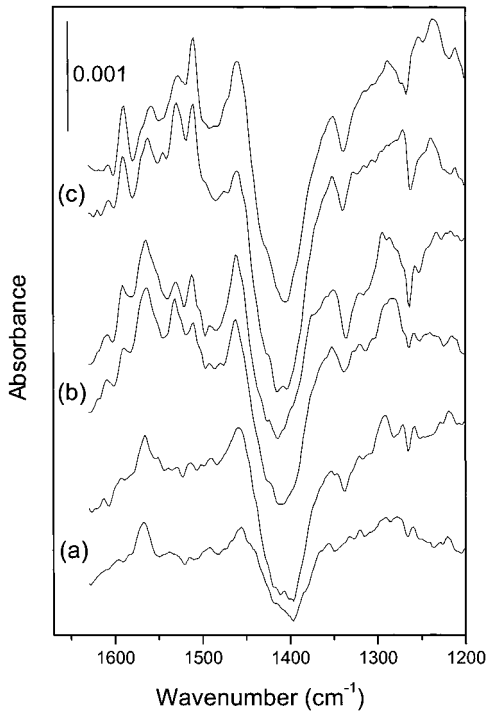

Figure 3. ATR spectra of cinchonidine on Pt/Al_2O_3-coated Ge crystal adsorbed from H_2-saturated CH_2Cl_2. C_{CD}: (a) 10^{-6} M, (b) 10^{-5} M, and (c) 10^{-3} M. Spectra are taken at 20 (lower trace) and 120 min time on stream.

with hydrogen. Due to strong absorption of the Al_2O_3 the noise increases drastically below 1000 cm^{-1}. Figure 2 (traces b−d) displays spectra of the very early stages of adsorption recorded by co-adding 20 scans at 4 cm^{-1} resolution. After 40 s contact time (trace b) two signals at 1567 and 1530 cm^{-1} are discernible together with a feature at around 1460 cm^{-1}. After 2 min (trace e) the ATR spectrum exhibits the major signals of cinchonidine but with changed relative intensity with respect to the solution spectrum. The signal at 1530 cm^{-1}, which is missing in the spectrum of dissolved cinchonidine, is most pronounced. However, at longer contact time the signals at 1590 and 1511 cm^{-1} become stronger at the expense of the 1530 cm^{-1} band.

Figure 2 also displays spectra recorded when N_2-saturated solvent was flown over the Pt/Al_2O_3 film after cinchonidine adsorption (traces l and m). Interestingly, the signals at 1567 and 1530 cm^{-1} remained, and the one at 1460 cm^{-1} was attenuated by the solvent flow, indicating that adsorption is irreversible for the species associated with these signals. On the other hand the signals at 1590 and 1511 cm^{-1} completely disappeared (trace m).

The time-dependent behavior of the signals between 1650 and 1450 cm^{-1} suggests that different species contribute to the spectrum of the alkaloid on the Pt surface. With the term species we will refer in the following to different adsorption geometries. To get more insight into the nature of these species we lowered the concentration of cinchonidine to 10^{-5} and 10^{-6} M. Results are shown in Figure 3. ATR spectra were recorded after 20 and 120 min contact time. Figure 3a shows that at the lowest concentration (10^{-6} M) a signal at 1572 cm^{-1} (shifting to 1567 cm^{-1} with increasing contact time) dominates the spectra together with the signal at 1458 cm^{-1}. With increasing concentration (traces b and c) additional signals at 1610, 1590, 1530, and 1511 cm^{-1} were observed. The band at ca. 1570 cm^{-1} is clearly composed of two signals. At higher concentration this band is slightly red-shifted, and its intensity is attenuated. Time evolution of the signals becomes less important at low concentration. For example, at a concentration of 10^{-3} M the signals at 1530 and 1511 cm^{-1} partially interchanged their intensity with adsorption time, which is less pronounced at 10^{-5} M. At high concentration (10^{-4}−10^{-3} M) a species associated with the strong signals at 1590 and 1511 cm^{-1} became dominant with a spectrum resembling the solution spectrum of the alkaloid. However, it should be noted that these signals arise from a species at the solid−liquid interface and not from the bulk solution, since the signals from dissolved cinchonidine are too small to be detected at these concentrations.

According to the time- and concentration-dependent spectra presented in Figures 2 and 3, at least three sets of signals can be distinguished, corresponding to three different species of cinchonidine adsorbed on Pt/Al_2O_3. It is also evident that the abundance of the different species changes with coverage. At low concentration (coverage) a single signal at 1567 cm^{-1} dominates, associated with a strongly adsorbed species. At higher (but still very low) concentration a second signal appears at 1530 cm^{-1}, associated with a second strongly adsorbed species. A species with a solution-like spectrum is observed when the concentration is further raised. The signal at 1511 cm^{-1}, which is slightly blue-shifted ($\Delta\nu = 2$ cm^{-1}) with respect to the position observed in solution, appears together with the signals at 1610, 1590, and 1570 cm^{-1}. The close spectral resemblance between the spectrum of this species and dissolved cinchonidine and the fact that this species is removed by the N_2-saturated solvent flow show that it is only weakly adsorbed.

When adsorption was carried out on Pt/Al_2O_3 from N_2-saturated solvent (not shown) but after cleaning of the metal surface with hydrogen, ATR spectra were dominated by the

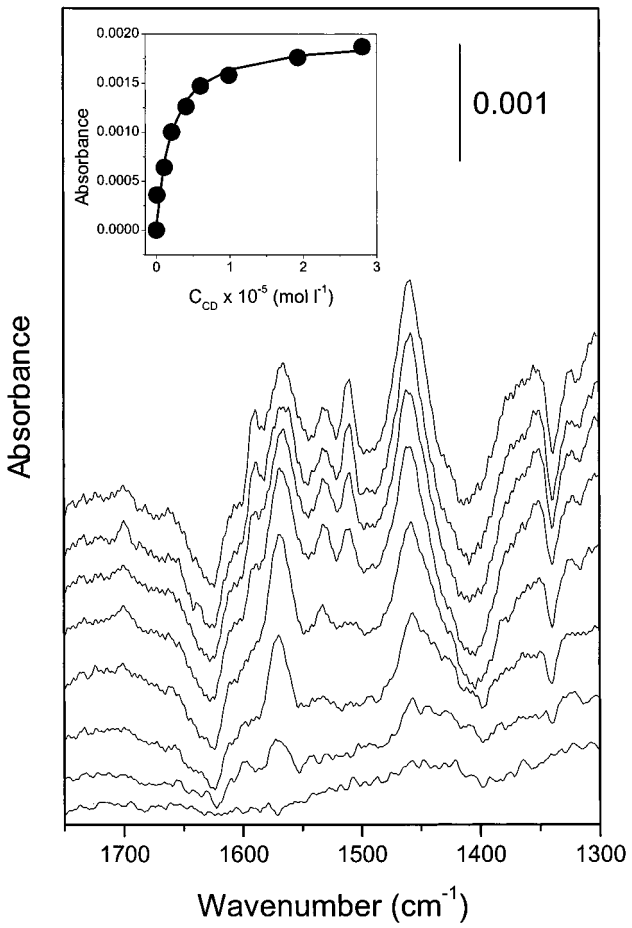

Figure 4. ATR spectra of cinchonidine on Pt/Al_2O_3 at 283 K recorded at increasing concentration ($0-3 \times 10^{-5}$ M). The inset shows the absorbance of the 1458 cm^{-1} signal as a function of cinchonidine concentration. The solid line represents a Langmuir-type adsorption model.

strong signal at 1530 cm^{-1}. The other mentioned signals were rather weak. The subsequent N_2-saturated solvent flow resulted in the features at 1570 and 1530 cm^{-1}. No significant time dependence of the signals was observed in contrast to that obtained from the experiments in the presence of H_2 (Figures 2 and 3).

Adsorption from a 10^{-4} M solution in cyclohexane (Figure 2n) followed the same trends as adsorption from CH_2Cl_2 showing signals at 1591, 1570, 1529, 1510, and 1460 cm^{-1}. Only two signals were observed at 1570 and 1529 cm^{-1} when adsorption was followed by solvent flow, indicating removal of the weakly adsorbed species. Further signals were visible at 1421, 1355, 1318, and 1270 cm^{-1} both during adsorption and following solvent flow. Except for the latter band, these signals are also present in the spectrum recorded in CH_2Cl_2 but are partially masked by the negative signals at 1400 and 1338 cm^{-1}.

Adsorption Isotherm. Figure 4 presents ATR spectra obtained at increasing concentration. The inset of Figure 4 shows the absorbance of the signal at 1458 cm^{-1}, which is common to all adsorbed cinchonidine species discussed above, as a function of concentration. Clearly this signal follows a saturation-like curve.

Assuming Langmuir type adsorption, the equilibrium constant for adsorption

$$CD + Pt \underset{k_{des}}{\overset{k_{ads}}{\rightleftharpoons}} CD - Pt$$

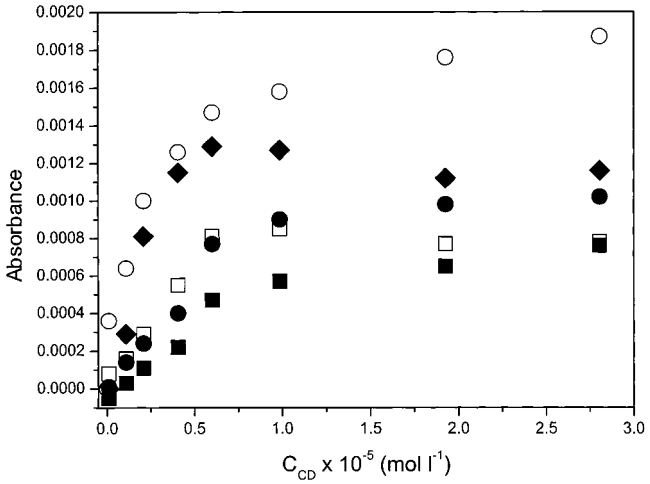

Figure 5. Absorbance (from spectra shown in Figure 4) of the signals at (○) 1458, (●) 1511, (□) 1530, (◆) ca. 1570 and (■) ca. 1590 cm^{-1} as function of cinchonidine concentration.

can be determined according to[36]

$$\frac{C_{CD}}{A} = \frac{C_{CD}}{A_{max}} + \frac{1}{A_{max}K_{CD}}$$

where C_{CD} is the concentration of cinchonidine in solution, A is the absorbance of the signal chosen as measure of the extent of adsorption, A_{max} is the absorbance at saturation, and K_{CD} is the adsorption constant. This treatment assumes that absorbance is proportional to coverage. From a plot of C_{CD}/A versus concentration an equilibrium constant K_{CD} of $5.1 \times 10^5 \pm 10^5$ M^{-1} corresponding to a Gibbs free energy of 31 ± 0.48 kJ/mol is obtained for cinchonidine adsorption on the Pt model catalyst at 283 K in CH_2Cl_2. The given errors have been determined from a fit of the data to the above equation. The line in the inset of Figure 4 results from the Langmuir adsorption model using the determined equilibrium constant. As can be seen the absorbance fits well to the Langmuir model. It should, however, be noted that the given value for the Gibbs free energy is an average over all of the species contributing to the 1458 cm^{-1} signal.

Figure 4 again demonstrates the discussed signal evolution with coverage and hence the presence of several species. Also, the slight red-shift of the signal at around 1570 cm^{-1} is evident. Also note the concentration dependence of the negative signals at 1338, 1400, and 1625 cm^{-1} due to removed ethylidyne ($\equiv C-CH_3$), $=CH_2$, and water from the interface. Figure 5 gives the maximum absorbance of the main signals in Figure 4 as function of cinchonidine concentration. The signals at 1511 and ca. 1590 cm^{-1} steadily increase with concentration, whereas the signals at 1530 and ca. 1570 cm^{-1} are slightly attenuated above 10^{-5} M. An analogous behavior can be seen with adsorption time (Figures 2 and 3).

Theoretical Results and IR Spectra of Cinchonidine, Quinoline, and Quinuclidine. Even though little is reported on the vibrational spectrum of the alkaloid this can be easily related to the spectra of its composing groups, quinoline and quinuclidine (Scheme 1).[37-40] The 1700−1500 cm^{-1} spectral

(36) Adamson, A. W. *Physical Chemistry of Surfaces*, 5th ed.; Wiley: New York, 1990.
(37) Katritzky, A. R.; Jones, R. A. *J. Chem. Soc.* **1960**, 2942.
(38) Brüesch, P.; Günthard, H. H. *Spectrochim. Acta* **1966**, *22*, 877.
(39) Wait, S. C.; McNerney, J. C. *J. Mol. Struct.* **1970**, *34*, 56.
(40) Srivastava, S. L.; Prasad, M.; Rohitashava *Spectrochim. Acta* **1984**, *40A*, 681.

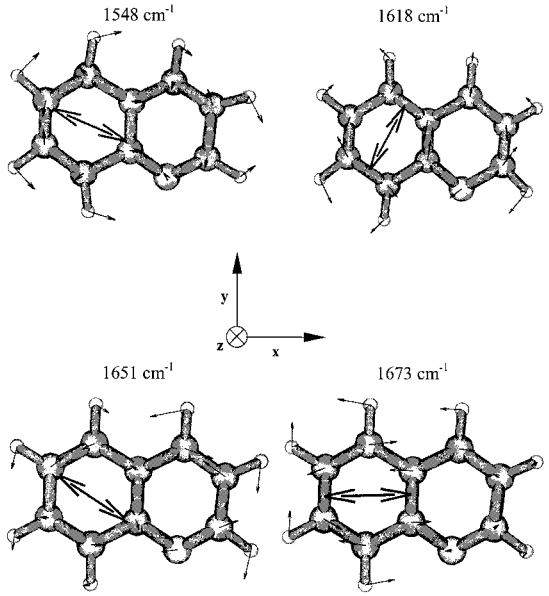

Figure 6. Pictorial representation of some vibrational modes of quinoline used to identify adsorption orientation. Arrows indicate atomic displacement vectors and direction of the dynamic dipole moment. The vibrations represent normal modes calculated at the completely optimized structure of the molecule (see text for details). The calculated harmonic frequencies are also given.

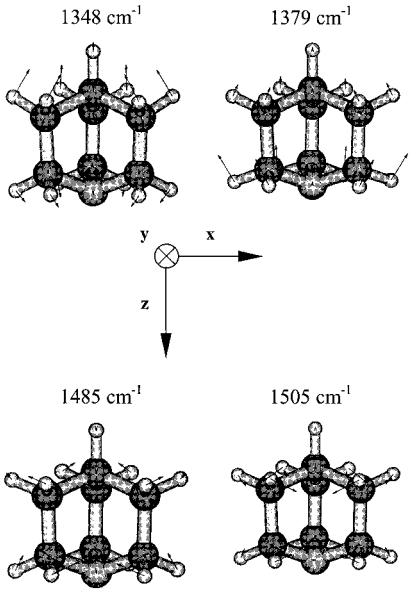

Figure 7. Pictorial representation of some of the vibrational modes of quinuclidine. Arrows indicate atomic displacement vectors of the calculated normal modes (see text for details). The calculated harmonic frequencies are also given.

region of cinchonidine has been assigned by analogy to the quinoline spectrum.[41,42] However, a more detailed analysis of the vibrational modes of the quinoline and quinuclidine moieties is needed here. In particular the direction of the dynamic dipole moment associated with the vibrational modes is important in view of the selection rule for adsorbates on metal surfaces.[43−45] Vibrational analysis is restricted here to modes in the 1650−1300 cm^{-1} spectral region.

IR Spectrum of Cinchonidine. An ATR spectrum of cinchonidine in CH_2Cl_2 measured over the bare Ge IRE showed signals at 3600 (ν(O−H)), 3043, 2942, and 2866 (ν(C−H)), 1635, 1615, 1592, 1571, 1509, 1463, 1424, 1386, 1346, 1322, 1279, 1236, 1163, 1139, 1093 (ν(C−O) + γ(O−H)), 1047, and 995 cm^{-1}. Table 1 gives the assignments of the vibrational modes of dissolved cinchonidine (transmission spectrum) in the 1650−1300 cm^{-1} range by comparison with the quinoline and quinuclidine spectra and ab initio calculations. The vibration at 1424 cm^{-1} belonging to the quinoline moiety was not observed in the transmission spectrum due to the interference with the solvent. For the region below 1300 cm^{-1} most of the vibrations are assigned to the quinoline moiety except for the signal at 1047 cm^{-1} which is probably common also to quinuclidine. The signal at 995 cm^{-1} is associated with the quinuclidine part.[38] A previous assignment of the Raman spectrum for an aqueous solution of cinchonine (the pseudoenantiomer of cinchonidine) hydrochloride is in good agreement with our data.[41]

IR spectrum of Quinoline and Quinuclidine. Figures 6 and 7 display some calculated normal modes of quinoline and quinuclidine, respectively. Arrows indicate the atomic displacement vectors. Quinoline belongs to the C_s point group. The main vibrations in the 1650−1500 cm^{-1} spectral range have all been assigned to ring stretching modes having A_1 symmetry.[39,40] Out-of-plane vibrations are found only below 1000 cm^{-1}. In a coordinate system defined as in Figure 6 the ring modes calculated at 1548 and 1618 cm^{-1} are mainly composed of out-of-phase and in-phase vibrations, respectively, of the C−C bonds parallel to the *y*-axis. A C−N stretch strongly contributes to the 1618 cm^{-1} mode. The calculated direction of the dynamic dipole moment for the various vibrations, that is the change of the molecular dipole moment along the normal coordinate, are also indicated in Figure 6. The two modes at 1548 and 1618 cm^{-1} are polarized roughly along the long and short axis of the molecule, respectively. The ring stretching modes calculated at 1651 and 1673 cm^{-1} are more localized on the N-containing ring and on the N-free ring, respectively.

Quinuclidine belongs to the C_{3v} point group.[38] The calculated IR spectrum shows four totally symmetric modes at 1505, 1485, 1379, and 1348 cm^{-1} in the 1700−1200 cm^{-1} range associated with C−H vibrations. These vibrations induce a dynamic dipole moment along the *z*-axis (Figure 7). Apart from the very strong C−H stretching modes the experimental IR spectrum of quinuclidine is dominated by signals at 1454 and 1320 cm^{-1}, which are doubly degenerated modes (calculated at 1489 and 1353 cm^{-1}, respectively). Weaker signals are found at 1377, 1353, and 1345 cm^{-1} together with a shoulder at 1463 cm^{-1} of the 1454 cm^{-1} band. The signal at 1377 cm^{-1}, which is not found in the calculation, is assigned to an overtone of a skeletal mode having *e* symmetry in Fermi resonance with the modes at 1345 and 1353 cm^{-1}.[38]

Adsorption of Quinoline, 2-Methylquinoline, and Quinuclidine. Quinoline, 2-methylquinoline and quinuclidine were separately adsorbed on evaporated Pt/Al_2O_3 films under the same conditions as used for cinchonidine. The results are shown in Figures 8 and 9 in which also transmission spectra of neat quinoline and a 0.01 M solution of quinuclidine in CH_2Cl_2, respectively, are given. Calculated spectra for quinoline and quinuclidine have also been included for comparison. The calculated harmonic frequencies are 2−3% too high, but the calculated intensity pattern fits very well the measured transmission spectra, thus allowing an unambiguous assignment.

(41) Weselucha-Birczynska, A.; Nakamoto, K. *J. Raman Spectrosc.* **1996**, *27*, 915.
(42) Ferri, D.; Bürgi, T.; Baiker, A. *J. Chem. Soc., Perkin Trans. 2* **1999**, 1305.
(43) Francis, S. A.; Ellison, A. H. *J. Opt. Soc. Am.* **1959**, *49*, 131.
(44) Greenler, R. G. *J. Chem. Phys.* **1966**, *44*, 310.
(45) Pearce, H. A.; Sheppard, N. *Surf. Sci.* **1976**, *59*, 205.

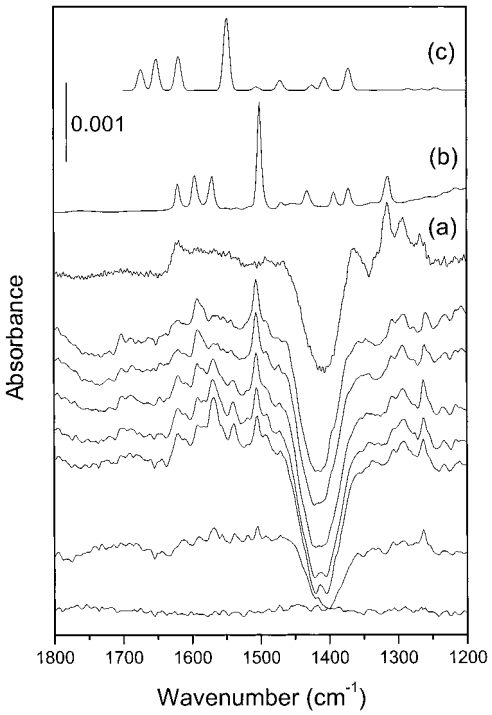

Figure 8. ATR spectra of quinoline (Q) on Pt/Al_2O_3-coated Ge crystal adsorbed from H_2-saturated CH_2Cl_2. Conditions: $C_Q = 10^{-3}$ M; $T =$ 283 K. Spectra recorded after (from bottom to top) 0, 2, 10, 20, 40, 80, and 120 min contact time are shown. (a) 2-methylquinoline on Pt/Al_2O_3 under the same conditions; (b) Scaled transmission spectrum (1:400; neat quinoline); (c) calculated spectrum.

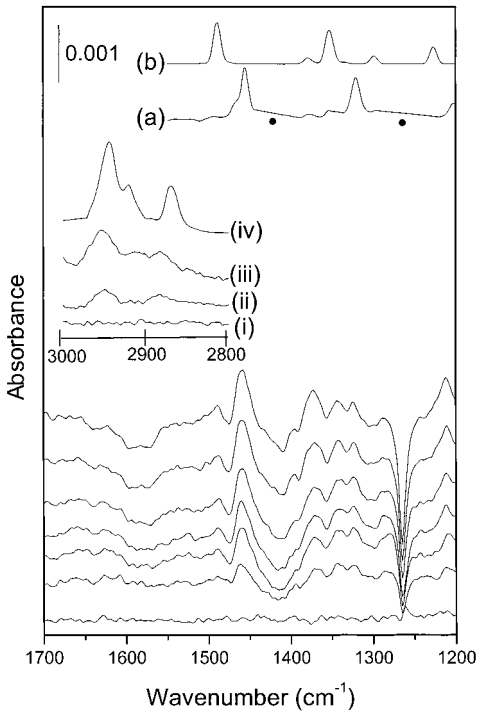

Figure 9. ATR spectra of quinuclidine (Qd) on Pt/Al_2O_3-coated Ge crystal adsorbed from H_2-saturated CH_2Cl_2. Conditions: $C_{Qd} = 10^{-3}$ M; $T =$ 283 K. Spectra recorded after (from bottom to top) 0, 2, 10, 20, 40, 80, and 120 min contact time are shown. The inset shows the 3000−2800 cm^{-1} spectral region with spectra taken at (i) 0, (ii) 2, and (iii) 120 min during adsorption and (iv) scaled (1:300) transmission spectrum of quinuclidine. (a) Scaled transmission spectrum (1:100; $C_{Qd} = 0.01$ M in CH_2Cl_2; uncompensated solvent (●)); (b) calculated spectrum.

ATR spectra of quinoline on Pt/Al_2O_3 show time dependence (Figure 8). At low contact time (<10 min) signals at 1620, 1592, 1569, 1540, and 1507 cm^{-1} are observed. The signals at 1569 and 1540 cm^{-1} are attenuated and almost disappear with increasing contact time while the signals at 1592 and 1507 cm^{-1} become stronger in a very similar way as the corresponding cinchonidine signals. The peak at 1507 cm^{-1} is relatively sharp and blue shifted with respect to neat quinoline ($\Delta\nu = 7$ cm^{-1}). The time-dependent behavior of the signals suggests that also for quinoline more than one species is present on the Pt surface. Furthermore, the spectrum of the ring vibrations of adsorbed cinchonidine and quinoline and its time (coverage) dependence is very similar, indicating similar adsorption behavior for the two molecules. This, in turn, shows that cinchonidine adsorption is dominated by the quinoline moiety. However, the time evolution, that is attenuation of the signals at about 1570 and 1530 cm^{-1}, is faster for quinoline than for cinchonidine.

In contrast to quinoline ATR spectra of adsorbed 2-methylquinoline (Figure 8a) showed distinct signals only at 1314 and 1294 cm^{-1} together with a broad signal at around 1620 cm^{-1}. Adsorption was, however, confirmed by the negative signals observed at 1400 and 1338 cm^{-1}. The absence of significant changes of the spectrum with time suggests that the adsorption mode of 2-methylquinoline is not affected by coverage.

When quinuclidine was contacted with the Pt film ATR spectra (Figure 9) displayed a strong and rather broad signal at 1461 cm^{-1}, together with bands at 1372, 1341, and 1323 cm^{-1}. All these features are assigned to quinuclidine according to Table 1. A weak signal on the high-frequency side of the main band was also observed at 1489 cm^{-1}. The strong C−H stretching vibrations, which are slightly blue-shifted with respect to the solution spectrum can also be observed (inset in Figure 9). Comparison between the solution spectrum and the spectrum of adsorbed quinuclidine shows that the relative band intensity drastically changes upon adsorption. In particular, the bands at 1372 and 1341 cm^{-1} are significantly enhanced for adsorbed quinuclidine. On the basis of the calculations the observed intensities of the bands is consistent with adsorption through the N lone pair, affording species oriented preferentially perpendicular to the metal surface, therefore enhancing A_1 modes, in agreement with data reported for quinuclidine on Pt/Al_2O_3 catalysts.[46]

Adsorption of 1THQ, 5THQ, and DHQ. Cinchonidine undergoes several steps of hydrogenation on the Pt catalyst under reaction conditions.[47] After fast hydrogenation of the vinyl moiety affording 10,11-dihydrocinchonidine[48] hydrogenation further proceeds, leading to a series of products in which the quinoline moiety is partially or completely hydrogenated. To exclude that (part of) the signals in the spectra shown in Figures 2, 3, 4, and 8 are due to hydrogenation products, we studied the interaction of potential hydrogenation products with the Pt/Al_2O_3 film. Figure 10 shows the ATR spectra obtained when 10^{-3} M solutions of 1THQ, 5THQ, and DHQ were contacted with the cleaned Pt surface, together with the transmission spectra of the neat materials. Comparison with Figures 2 and 8 clearly shows that none of the quinoline derivatives displays the sets of signals observed on adsorption of cinchonidine or quinoline.

(46) Brönnimann, C.; Bodnar, Z.; Aeschimann, R.; Mallat, T.; Baiker, A. *J. Catal.* **1996**, *161*, 720.
(47) Morawsky, V.; Prüsse, U.; Witte, L.; Vorlop, K. D. *Catal. Commun.* **2000**, *1*, 15.
(48) Talas, E.; Botz, L.; Margitfalvi, J.; Sticher, O.; Baiker, A. *J. Planar Chromatogr.-Mod. TLC* **1992**, *5*, 28.

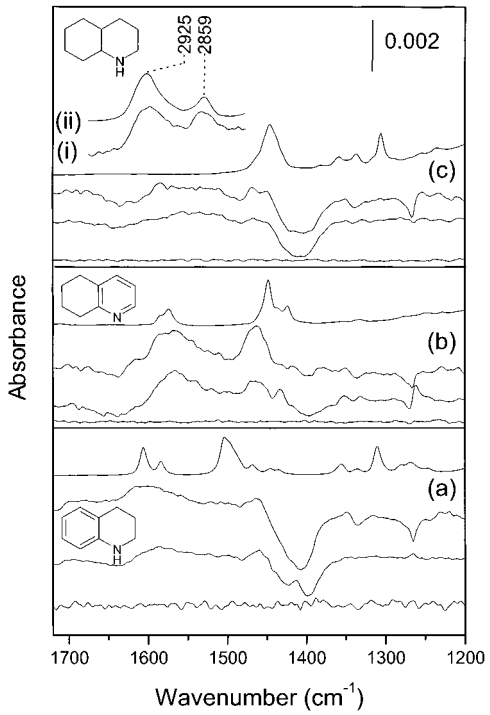

Figure 10. ATR spectra of 1-THQ, 5-THQ, and DHQ on Pt/Al_2O_3-coated Ge crystal adsorbed from H_2-saturated CH_2Cl_2. Conditions: $C = 10^{-3}$ M; $T = 283$ K. Spectra are taken at 0, 4 (2 for DHQ), and 120 min time on stream. Transmission spectra of (a) 1-THQ (1:500), (b) 5-THQ (1:200), and (c) DHQ (1:100) as neat liquids are also presented. The inset for DHQ shows the 3000−2800 cm^{-1} spectral range: (i) ATR spectrum after 120 min of time on stream and (ii) transmission spectrum of neat DHQ (1:500).

Removal of Solvent and Solvent Decomposition Products from the Interface. Usually infrared spectra, and also the spectra reported here, are relative measurements, that is *changes* in, for example, reflectivity with respect to the reference give rise to signals. Therefore removal of species that were present during measurement of the reference will give negative signals. Apart from the positive signals originating from cinchonidine adsorption on Pt/Al_2O_3 the spectra in Figure 2 show negative bands also common to Figures 1, 3, 8, 9, and 10. These bands are found at ca. 1630, 1400, 1338, and ca. 1260 and at 1120 cm^{-1} (not shown) with varying intensities according to the nature of the adsorbed molecule. The weak feature observed at around 1630 cm^{-1} is attributed to water removal from the Pt/solution interface. The negative signal at 1400 cm^{-1} is due to removal of methylene ($=CH_2$) species arising from the decomposition of CH_2Cl_2 solvent on Pt/Al_2O_3 as described above. As previously reported the peaks at 1338 and 1120 cm^{-1} are attributed to ethylidyne adsorbed on Pt, likely formed by recombination of methylene.[27] Pt is an active catalyst for hydrodechlorination of organochlorinated compounds and CH_x fragments can be generated.[49] The formed $=CH_2$, associated with the broad negative band at 1400 cm^{-1}, can combine on the catalyst producing ethylidyne ($\equiv C-CH_3$) that is the most stable C_2 hydrocarbon on Pt under hydrogenation conditions.[50] The signal at ca. 1260 cm^{-1} arises from incomplete compensation of a strong CH_2Cl_2 vibration. A negative band thus indicates the displacement of solvent from the solid−liquid interface on adsorption of "bulky" molecules.

Quinoline and cinchonidine behave in a very similar way concerning displacement of $=CH_2$, $\equiv C-CH_3$, and CH_2Cl_2 upon adsorption on Pt. On the other hand the effects of quinuclidine adsorption is different. The band around 1400 cm^{-1} is significantly weaker, whereas the sharp negative feature at around 1260 cm^{-1} is quite strong. This behavior has probably to be attributed to the size and shape and the different adsorption behavior of these molecules.

The features at around 2000 (Figure 2, traces p−r) and 1750 cm^{-1} (Figure 2, traces a−m) are associated with CO. The peculiar shape of the bands indicates that CO is preferentially removed (displaced) from specific sites, while some CO is formed on others. Since the behavior of the CO features was the same for cinchonidine and quinoline, we conclude that CO does not form from decomposition of cinchonidine (which contains an O−H group). CO formation and removing has also been observed for pyridine, 1THQ, 5THQ, and DHQ. Since CO is a very strong IR absorber and CO signals were always small (ca. 50 times smaller than typical signals from a saturated CO layer[27]), we can conclude that the absolute coverage of CO was rather low at any time during the experiment.

Discussion

Pyridine Adsorption. Pyridine adsorption in UHV is rather surface-sensitive. Several species can be observed according to the nature of the pyridine−metal bond. On Pt at low coverage a flat π-adsorption is favored, evolving into species with the molecular plane tilted or normal to the surface as the coverage increases.[51−53] Moreover, at around room temperature the symmetry of the pyridine adsorption complex reduces to C_1. On several metals including Pt at temperatures close to 300 K an α-pyridyl is formed by α-hydrogen abstraction (dissociation of C−H bond nearest to N).[52,54−57]

According to reported spectra[53] for pyridine on Pt(111) we can assign the observed ATR signals at 1601, 1485, 1440, 1218, 1068, and 1041 cm^{-1} in Figure 1 to pyridine adsorbed via the N lone pair forming a σ-bond with the Pt, that is with the molecular plane tilted with respect to the Pt surface. The signal at 1564 cm^{-1} can be assigned to α-pyridyl species. The observed attenuation of this signal with increasing contact time indicates that α-pyridyl is disfavored with respect to N lone pair bonded pyridine at high coverage. However, Figure 1 shows that even under reducing conditions it can be found as a minor species on the Pt/Al_2O_3 model catalyst at 283 K. On the other hand the fact that on neat solvent flow the signals of N lone pair bonded pyridine disappear indicates that the interaction via the N lone pair is weak. It should be noted that at room temperature pyridine adsorption on Pt/Al_2O_3 in the presence of solvent and hydrogen is remarkably different from adsorption in *vacuo* on Pt(111). In the former case both α-pyridyl and N lone pair bonded pyridine is observed, with the latter being the dominant species, whereas in UHV the α-pyridyl prevails.

Cinchonidine and Quinoline Adsorption. Slow hydrogenation of the aromatic moiety of cinchonidine occurs under high H_2 pressure,[18,47] leading to a remarkable attenuation of the

(49) Ordoñez, S.; Sastre, H.; Diez, F. V. *Appl. Catal., B* **2000**, *25*, 49.
(50) Wieckowski, A.; Rosasco, S. D.; Salaita, G. N.; Hubbard, A.; Bent, B. E.; Zaera, F.; Godbey, D.; Somorjai, G. A. *J. Am. Chem. Soc.* **1985**, *107*, 5910.
(51) Johnson, A. L.; Muetterties, E. L.; Stöhr, J.; Sette, F. *J. Phys. Chem.* **1985**, *89*, 4071.
(52) Grassian, V. H.; Muetterties, E. L. *J. Phys. Chem.* **1986**, *90*, 5900.
(53) Haq, S.; King, D. A. *J. Phys. Chem.* **1996**, *100*, 16957.
(54) Kishi, K.; Chinomi, K.; Inoue, Y.; Ikeda, S. *J. Catal.* **1979**, *60*, 228.
(55) DiNardo, N. J.; Avouris, P.; Demuth, J. E. *J. Chem. Phys.* **1984**, *81*, 2169.
(56) Mate, C. M.; Somorjai, G. A.; Tom, H. W. K.; Zhu, X. D.; Shen, Y. R. *J. Chem. Phys.* **1988**, *88*, 441.
(57) Jakob, P.; Lloyd, D. R.; Menzel, D. *Surf. Sci.* **1990**, *227*, 325.

enantiodifferentiating power of the modifier[58] attributed to the diminished adsorption strength. Comparison of Figures 2, 8, and 10 clearly shows that no hydrogenation product of the quinoline ring can be detected at the solid−liquid interface since none of the sets of signals of 1THQ, 5THQ, and DHQ can be found in the spectra of adsorbed cinchonidine and quinoline. On the other hand the absence of a band at 1635 cm^{-1} associated with the C═C stretching vibration of the vinyl moiety shows that cinchonidine does undergo hydrogenation at $C_{10}-C_{11}$ (Scheme 1). This observation is in accordance with the finding that the C═C double bond is hydrogenated fast.[48]

To our knowledge only few studies have been reported on the adsorption of quinolines on metal surfaces. A tilted orientation has been found on both Cu and Ag.[59,60] For comparison, pyridine shows a coverage-dependent behavior on Ag(111),[61] whereas it adsorbs with the molecular plane tilted with respect to the Cu(110) surface at all coverages.[53] According to this comparison it seems likely that adsorption of the two molecules is similar also on Pt where both coverage and temperature dependence are observed for pyridine.[51,53] Earlier H/D exchange studies seem to support this view.[62] Since the ATR spectra of cinchonidine and quinoline in the spectral region of the ring deformation modes show similar behavior, this would also hold for the alkaloid.

The ATR spectra shown in Figure 2 indicate that the adsorption process of cinchonidine is rather complex. At least three surface species can be distinguished, associated with (i) the signals at 1570 and 1460 cm^{-1}, (ii) the signals at 1570, 1530, and 1460 cm^{-1}, and (iii) the set of signals resembling the solution spectrum. This latter species is weakly adsorbed on Pt/Al_2O_3. Since very similar spectral behavior is observed for cinchonidine and quinoline, comparable adsorption behavior can be inferred for the two molecules. This indicates that the quinuclidine part of the alkaloid plays the dominant role in the adsorption process. However, signals associated with the quinuclidine part of cinchonidine are also evident in the spectra of adsorbed cinchonidine. The signals found below 1450 cm^{-1} in cyclohexane solvent are in fact attributable to both quinoline (1421 cm^{-1}) and quinuclidine (1355 and 1318 cm^{-1}) moieties according to Table 1. Inspection of Figures 2, 8, and 9 suggests that the signal at 1458 cm^{-1} associated with the quinuclidine group is common to all the three species. The contribution of several species to this band induces a slight shift of the band maximum, best seen in Figure 4, as the abundance of the species changes. Similarly, all three species may contribute to the band at around 1570 cm^{-1}, which slightly shifts to lower wavenumbers with increasing concentration, as it can be seen from Figures 3 and 4. However, the contribution to this band of the weakly bonded species having a solution-like spectrum is only marginal as a comparison between traces l and m in Figure 2 demonstrates. The feature at 1100 cm^{-1} (not shown in Figure 2) can be tentatively attributed to the C−O vibration of the OH group at C_9. The slight blue-shift with respect to the solution spectrum (1093 cm^{-1}) can arise from hydrogen bonding of the O−H group with the metal surface upon adsorption of the alkaloid. More about the nature of the adsorbed species of cinchonidine is learned by comparing spectra at changing concentration and by considering the results of the vibrational analysis of the quinoline moiety.

Assignment of the Spectra of Adsorbed Cinchonidine. ATR spectra of cinchonidine at very low concentration show only one distinct signal due to the quinoline ring at ca. 1570 cm^{-1}. This indicates strong orientation of the species associated with this band. Note that in solution (Figure 2o) the band at 1570 cm^{-1} does not belong to the strongest signals of the alkaloid. Figure 6 shows that the modes of quinoline calculated at 1618 and 1548 cm^{-1}, corresponding to the vibrations of cinchonidine at 1570 and 1509 cm^{-1} (1569, 1500 cm^{-1} for quinoline, Table 1) are polarized preferentially along the *y*- and *x*-axis, respectively. According to the metal surface selection rule[44] these vibrations can be observed only if the *y*- and *x*-axis, respectively, are tilted with respect to the metal surface. The signal at ca. 1570 cm^{-1} is therefore attributed to a species with the *x*-axis of the quinoline moiety predominantly parallel to the surface with a degree of tilting of the *y*-axis possibly because the quinoline N slightly points toward the surface. Such an orientation and the fact that the species is strongly adsorbed are consistent with a π-bonded species. The slight tilting of the quinoline moiety is also consistent with the relatively small shift of the signal at ca. 1570 cm^{-1} with respect to the solution spectrum. Note, that although only one weak band in the 1500−1600 cm^{-1} region is observed for this species, considerable adsorption is confirmed by the negative peaks associated with removal of solvent decomposition products, as best seen in Figure 3a.

On the other hand, the weakly adsorbed species associated with the signals at 1610, 1590, and 1511 cm^{-1} must be strongly tilted. We assign these signals to species that are weakly adsorbed through the quinoline N lone pair. It is known for pyridine that adsorption through the N lone pair results in a slight blue-shift of some ring vibrations in which the C−N bond is involved. In fact a blue-shift, although small, is also observed for the signal centered at 1500 cm^{-1} in quinoline and 1509 cm^{-1} in cinchonidine.

We have previously assigned the signal at 1530 cm^{-1} to cinchonidine strongly adsorbed via the quinoline N in a tilted orientation.[28] On the basis of several experimental observations we can more precisely assign the band to a species where the H in α-position to the quinoline N has been abstracted. This species will be called in the following α-quinolyl, for analogy with the α-pyridyl found on Pt. The C−Pt bond of α-quinolyl leads to a strong adsorption bond and a tilted orientation of the quinoline moiety of cinchonidine. Figure 1 shows that the signal associated with α-pyridyl at 1564 cm^{-1} is attenuated with time. It seems that the α-pyridyl is easily rehydrogenated and that at high coverage it is disfavored with respect to the N lone pair bonded species. Figure 2 shows that the 1530 cm^{-1} band shows similar time dependence. In fact, interconversion of the intensity of the bands associated with the α-H abstracted and N lone pair bonded species is similar for pyridine, quinoline, and cinchonidine as shown in Figures 1, 2, and 8. The most diagnostic vibration of α-pyridyl on Pt at 1564 cm^{-1} corresponds to the 1598 cm^{-1} vibrational mode of N lone pair bonded pyridine.[52,53] Hence, for pyridine α-abstraction leads to a red-shift of 34 cm^{-1} for this vibration. A similar shift of 30−40 cm^{-1} of the corresponding bands is also found for cinchonidine (1570, 1530 cm^{-1}) and quinoline (1569, 1540 cm^{-1}) upon α-H abstraction.

Adsorption of cinchonidine from N_2-saturated solvent gave predominantly α-quinolyl because re-hydrogenation is not

(58) Blaser, H. U.; Jalett, H. P.; Monti, D. M.; Baiker, A.; Wehrli, J. T. *Stud. Surf. Sci. Catal.* **1991**, *67*, 147.
(59) Fleischmann, M.; Hill, I. R.; Sundholm, G. *J. Electroanal. Chem.* **1983**, *158*, 153.
(60) Chowdhury, J.; Ghosh, M.; Misra, T. N. *J. Colloid Interface Sci.* **2000**, *228*, 372.
(61) Demuth, J. E.; Christmann, K.; Sanda, P. N. *Chem. Phys. Lett.* **1980**, *76*, 201.
(62) Calf, G. E.; Garnett, J. L.; Pickles, V. A. *Aust. J. Chem.* **1968**, *21*, 961.

possible and the absence of hydrogen favors the formation of the α-quinolyl. On the other hand, if the α-H is substituted with a methyl group, as in 2-methylquinoline, formation of the α-quinolyl is hindered. Accordingly, the ATR spectrum shown in Figure 8a does not show a signal at around 1530 cm^{-1}, supporting the assignment of the signal at 1530 cm^{-1} to a α-quinolyl species. Since the spectra of cinchonidine (and quinoline, respectively) and 2-methylquinoline appear much different in the 1600−1400 cm^{-1} spectral range, the adsorption mode of these molecules must be different. For 2-methylquinoline the presence of the methyl group hinders the interaction of the N lone pair with the Pt surface and hence a tilting of the aromatic moiety with respect to the surface. Adsorption occurs more likely with the molecular plane parallel to the metal surface. This is supported by the absence of strong bands in the 1500−1600 cm^{-1} region.

Results obtained for cinchonidine adsorption on Pd/Al_2O_3 instead of Pt/Al_2O_3 thin films further support the assignment of the 1530 cm^{-1} band.[63] C−H cleavage to form α-pyridyl has not been observed on Pd under UHV conditions in contrast to Pt, thus showing that α-abstraction is disfavored on Pd with respect to Pt.[64] Accordingly, the signal at 1530 cm^{-1} could hardly be detected in the ATR-IR spectra of cinchonidine adsorbed on Pd/Al_2O_3 under identical conditions as used for adsorption on Pt/Al_2O_3.

Interconversion between Different Cinchonidine Adlayers. Careful inspection of the spectra in Figure 2 shows that the weakly N lone pair adsorbed species and α-quinolyl species are not independent of each other, which is best seen by comparing the bands at 1530 (α-quinolyl) and 1510 cm^{-1} (N lone pair bonded) in Figures 2 and 3. The intensity of these two bands is anti-correlated. At the initial stages of adsorption (Figure 2) and at low concentration (Figure 3) the 1530 cm^{-1} band is strong and the 1510 cm^{-1} band weak. With increasing time (Figure 2) and concentration (Figure 3) the 1510 cm^{-1} band becomes stronger at the expense of the 1530 cm^{-1} band. When there is neat solvent flow, the opposite behavior is then observed, leaving at the end only the band at 1530 cm^{-1}. This behavior suggests that the two species compete for the same Pt sites and are interconverted one into the other with the concentration of cinchonidine and the hydrogen being the driving force for the interconversion. Furthermore, the fast removal of N lone pair bonded species with the neat solvent flow suggests a fast dynamic equilibrium between these surface species and dissolved molecules. On the other hand, Figure 2 indicates that the transition from a less crowded surface with predominantly α-quinolyl to a more crowded surface with predominantly N lone pair bonded cinchonidine is slow, whereas the reverse process is fast. As mentioned above, the time evolution of the signals is faster for quinoline than for cinchonidine. It is likely that the presence of the quinuclidine moiety in cinchonidine affects the kinetics of surface crowding with respect to quinoline.

During the transition from α-quinolyl to N lone pair bonded cinchonidine the intensity of the negative signal at 1400 cm^{-1} associated with $=CH_2$ species from solvent decomposition stays almost constant. This indicates that the surface area covered by the different adlayers is constant and hence also the area remaining for solvent decomposition products. On the other hand, the negative signal at 1264 cm^{-1} from the solvent seems more pronounced for the adlayer with a high fraction of N lone pair bonded cinchonidine as best seen in Figure 3. Hence, the adlayer with more N lone pair bonded species has a larger volume, which would be expected for a more densely packed adlayer.

Scheme 2. Suggested Adsorption Mechanism of Cinchonidine on Pt/Al_2O_3 at 283 K Based on ATR Experiments[a]

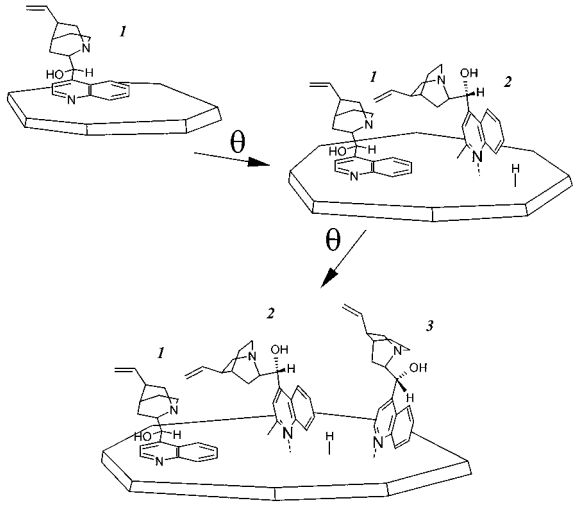

[a] θ represents the surface coverage. Species ***1***: π-bonded, ***2***: α-H Abstracted and ***3***: N lone pair bonded

Adsorption Mechanism. On the basis of the above discussion we propose an adsorption mechanism as pictorially shown in Scheme 2. At low coverage cinchonidine (and quinoline) adsorbs on the Pt surface via the π-system in a predominantly but not completely flat orientation (***1***). As the available space on the surface becomes restricted, additional cinchonidine adsorbs in a tilted orientation by formation of α-quinolyl species (***2***) and N lone pair bonding (***3***). According to the ATR spectra ***2*** is more strongly bonded than ***3***. Also, ***1*** is more strongly bonded than ***2*** as it is clear from the spectra recorded at low concentration (Figure 4) since the signal at 1567 cm^{-1} appears before the one at 1530 cm^{-1}. On further increasing coverage interconversion between ***2*** and ***3*** eventually occurs. At this point all three different species ***1***, ***2***, and ***3*** of cinchonidine coexist on the surface.

It should be noted that the solvent may play an important role for the adsorption of cinchonidine. As it is shown in the ATR spectra and depicted in Figure 11 cinchonidine has to compete for adsorption sites with adsorbates resulting from solvent decomposition (Figure 11b−c). As demonstrated here for CH_2Cl_2 and cyclohexane the adsorbate layer that cinchonidine has to compete with is different for each solvent, which may be a critical factor for the observed strong solvent dependence of the enantioselective hydrogenation of α-functionalized ketones over cinchonidine modified Pt.

Implications for the Enantioselective Hydrogenation of Ethyl Pyruvate. It has been reported that the enantiomeric excess (ee) during the enantioselective hydrogenation of ethyl pyruvate to (*R*)-ethyl lactate on cinchona-modified Pt-based catalysts depends on several parameters. Among these the concentration of the modifier plays a major role.[11] In the case of cinchonidine a maximum ee is reached at a modifier concentration of less than 0.05 g/L (1.7×10^{-4} M), and a slight decrease of ee is observed for higher concentration.

The question arises, which of the adsorbed species is responsible for enantiodifferentiation? Although this question cannot be conclusively answered solely on the basis of the presented results, the observations are consistent with the

(63) Ferri, D.; Bürgi, T.; Baiker, A. Manuscript in preparation.
(64) Grassian, V. H.; Muetterties, E. L. *J. Phys. Chem.* **1987**, *91*, 389.

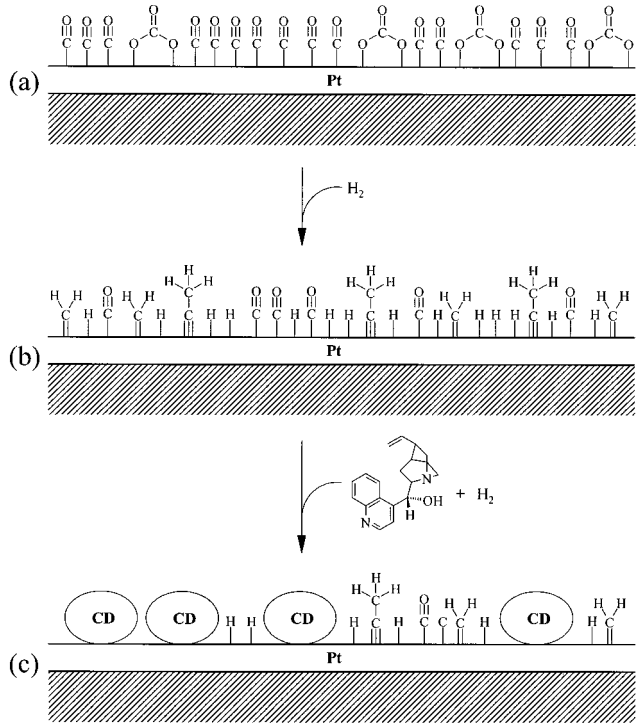

Figure 11. Pictorial representation of the composition of the adsorbate layer on Pt during (a) N_2-saturated solvent flow, (b) cleaning with H_2-saturated solvent, and (c) adsorption of cinchonidine (CD) in the presence of hydrogen.

proposal that the strongly adsorbed π-bonded species ***1*** is involved in enantiodifferentiation. As mentioned above the α-quinolyl species ***2*** was more abundant in the absence of hydrogen. Adsorbed hydrogen seems to disfavor this species, likely due to its hydrogenation. The species ***2*** is therefore expected to be less abundant on the Pt surface at high hydrogen pressure. The fact that the observed ee in the hydrogenation of ethyl pyruvate has a maximum at relatively high hydrogen pressure[65] indicates that ***2*** is not responsible for enantioselection. The N lone pair bonded species ***3*** on the other hand seems too weakly bonded to play an important role in enantiodifferentiation. However, its presence on the Pt surface could contribute to the drop in ee at high cinchonidine concentration.

Conclusions

The adsorption of the alkaloid cinchonidine on a Pt/Al_2O_3 model catalyst in the presence of solvent and hydrogen is strongly concentration (coverage)-dependent. The quinoline moiety of the molecule is responsible for adsorption. At very low concentration (around 10^{-6} M) cinchonidine adsorbs with the quinoline moiety in a predominantly but not completely flat orientation, likely via the π-aromatic system. As the surface gets crowded, additional cinchonidine molecules adsorb in a tilted orientation via α-H abstraction and N lone pair bonding. The latter species are only weakly adsorbed and in a fast dynamic equilibrium with dissolved cinchonidine. The α-H abstracted and π-bonded cinchonidine are strongly bound and remain adsorbed in the presence of neat solvent. A rather slow transition from adlayers with predominantly α-H abstracted to adlayers with predominantly N lone pair bonded species is observed, the driving force for this process being the cinchonidine concentration. A similar although faster transition is observed for quinoline, indicating that the quinuclidine part of cinchonidine affects the kinetics of surface crowding. The ATR spectra clearly demonstrate that cinchonidine has to compete with solvent decomposition products for adsorption sites on the Pt. The solvent decomposition products are different for various solvents. This observation may partly explain the strong solvent effect observed in the enantioselective hydrogenation of activated carbonyl compounds on cinchonidine-modified Pt.

Acknowledgment. We thank Professor A. Baiker for stimulating discussion. The financial support of ETH Zürich and the Swiss National Science Foundation and the grants of computer time by ETH Zürich and CSCS Manno are gratefully acknowledged.

JA011769U

(65) Meheux, P. A.; Ibbotson, A.; Wells, P. B. *J. Catal.* **1991**, *128*, 387.